

## Rolling Locomotion of a Deformable Soft Robot with Built-in Power Source

Yasuaki Matsumoto\*, Hisashi Nakanishi and Shinichi Hirai

*Department of Robotics, Ritsumeikan University,  
Kusatsu, Shiga 525-8577, Japan*

*\*E-mail: hirai@se.ritsumei.ac.jp*

*http://www.ritsumei.ac.jp/se/~hirai/*

Locomotion over rough terrain has been achieved mainly by rigid body systems, including crawlers and leg mechanisms. We have proposed an alternative method, which uses deformation of a robot body, and developed a prototype of this deformable robot. But, electric power was externally supplied, such that power supply cables hindered the locomotion of the robot. We describe here the rolling locomotion of a deformable soft robot with an internally supplied power source. We applied dynamic simulation with particle-based modeling to analyze the rolling motion of this robot and found that increased weight had little influence on the kinematic performance of this robot on flat surfaces. Increased weight, however, was effective in providing greater stability on slopes.

*Keywords:* rolling, deformation, soft robot, simulation.

### 1. Introduction

Locomotion over rough terrain has been achieved mainly by rigid body systems, including crawlers and leg mechanisms<sup>1</sup>. We have described an alternative method, one that uses deformation of a robot body<sup>2</sup>. Rolling of a soft robot is a novel form of locomotion. With soft actuators, this form of locomotion can be soft, light and safe, as well as being able to positively use the dynamic characteristics of a soft object<sup>3</sup>. We developed a prototype of this deformable robot. However, the electric power was externally supplied, such that power supply cables hindered the locomotion of this robot. We therefore developed a new form of soft robot, with a built-in power source, and assessed its rolling by simulation and experimentally.

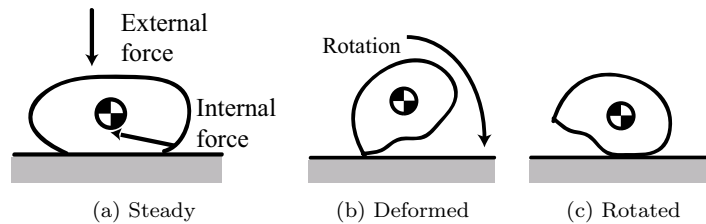


Fig. 1. Principle of rolling locomotion.

## 2. Principle of rolling locomotion

If a deformable circular body is stable on a horizontal surface on the ground, as in Fig. 1-(a), the gravitational potential energy of the body is at its minimum; i.e., the gradient of the energy with respect to the ground is equal to zero. If the body deforms, as in Fig. 1-(b), the deformation changes the gradient, generating a moment around the point of contact between the body and the ground due to the gravitational force. This moment may cause the body to roll along the ground, until it achieves the stable state shown in Fig. 1-(c). Repeated deformation of the body by actuators may enable the body to roll continuously along the ground.

## 3. Rolling soft robot

Figure 2 shows two robots, one (robot I) with an external power source and the other (robot II) with a built-in power source. Table 1 shows the specifications of these soft robots. Robot I consists of eight shape memory alloy (SMA) coil actuators attached to the inside of a circular shell made of spring steel and labeled A to H. Robot II includes three lithium polymer (Li-Po) batteries and a control circuit board, as shown in Fig. 2-(b). The control circuit board, built using a PIC microcontroller and field effect transistors (FET), measures  $24.5 \times 24.5 \times 2.5$  mm and weighs a total of 1.0 g. The battery, which measures  $12 \times 20 \times 3$  mm and weighs 0.8 g, has sufficient power to drive the SMAs. Moreover, the batteries were placed so as not to hinder the contraction of the SMAs and so that they balanced the robot center of gravity. The required power consumption of each SMA coil is 1.5 W. Robot I is driven by pulse width modulation (PWM) control, with an input of 6.0 V and a 30% duty ratio, whereas robot II has an input of 3.7 V and a 78% duty ratio. When voltage is applied to the coil, it contracts, causing the circular shell to deform. By applying an appropriate voltage pattern to the coils, the robot can roll continuously. As an example,

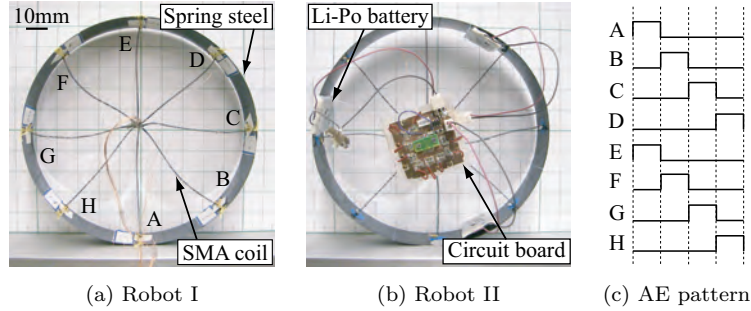


Fig. 2. Rolling soft robot and a pattern of SMA-contraction.

Table 1. Specification of soft robot.

Robot	Total mass (g)	Size (mm)	Spring steel thickness (mm)	$R_{flex}$ ( $N/m^2$ )
I	5.9	$\phi 100 \times 20$	0.10	0.34
II	10.7	$\phi 100 \times 20$	0.10	0.34

the order of SMA-contraction was arranged as in Fig. 2-(c), which we call an AE pattern. The switching time for each SMA is 5.0s, making the total driving time of robot II 180s for this AE pattern.

#### 4. Experimental result of rolling soft robot

In this section, we experimentally show the rolling of robots I and II on a horizontal surface and on a surface inclined 10 degrees. Each robot was driven with an AE pattern, and alternately switched at 5.0s. Initially the shape of the rolling robot was close to a perfect circle. The material of the floor was polyvinylchloride (PVC), with static coefficient of friction of 0.45. The ambient temperature during each experiment was 25 °C.

Figure 3 shows sequential snapshots of the rolling robot. Robots I and II were compared on horizontal ground and inclined ground while the robots had an oval shape. The oval shape was maintained constantly so that each robot would not slope down during the experiments.

Figure 4 shows the distance moved in these experiments. Stair-shaped locomotion is a characteristic of a rolling robot. The sharp rising response indicates the moment generated by the robot while transforming and rolling. To compare the two robots, we performed experiments testing the robots on a horizontal and an inclined surface. We found that robot

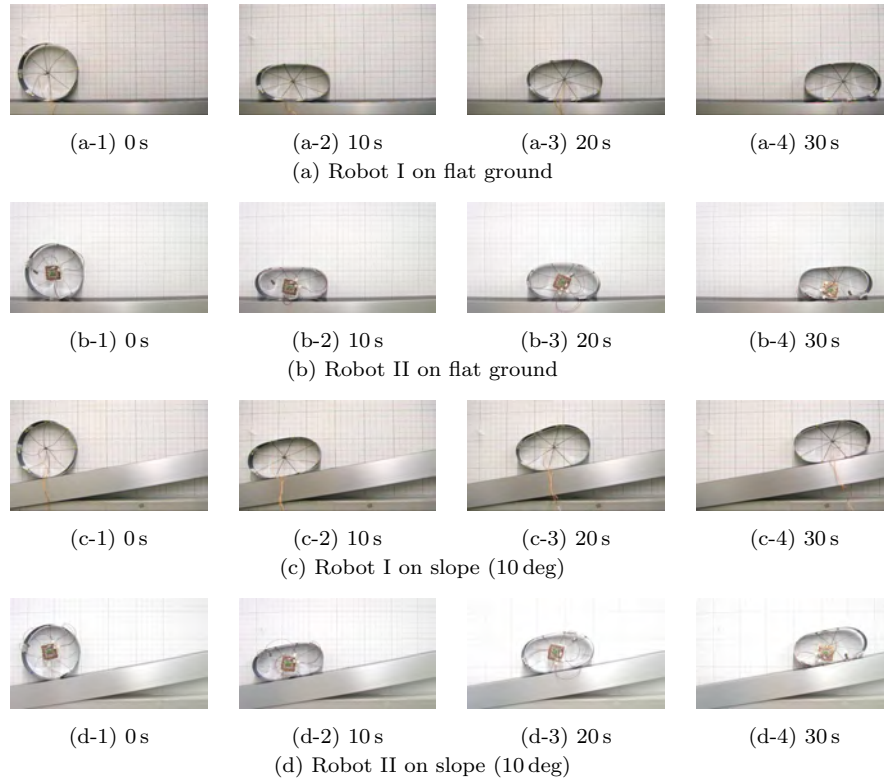


Fig. 3. Sequential snapshots of the rolling robot.

II was 4% slower on horizontal ground and 1% slower on inclined ground when compared with robot I. In contrast, robot II had a more stable and robust locomotion than robot I.

### 5. Simulation of rolling soft robot

The dynamic simulation of robots I and II using particle-based modeling was performed for two conditions, rolling motion on a horizontal surface and rolling motion on a slope. The main objective was to analyze the effect of robot weight on rolling.

The particle model <sup>2</sup> shown in Fig. 5 was employed, with a total of 81 mass points distributed throughout the body (64 points) and SMAs (17 points). In robot II, the weight of the battery and the circuit was included.

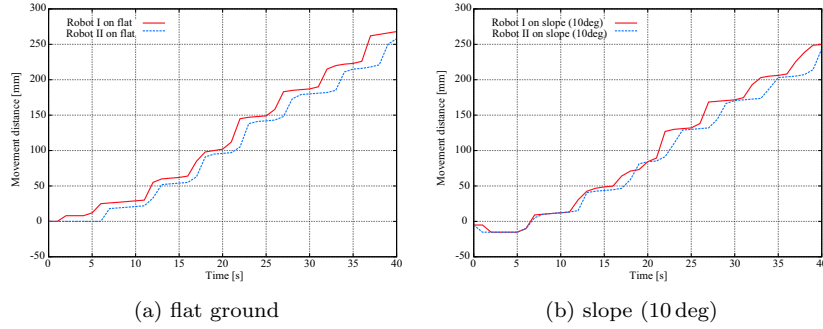


Fig. 4. Distance moved, as assessed experimentally.

We used the penalty method to express the reaction force and frictional force on the ground. As expressed, the generated force was related to the martensite and austenite transformations on SMA<sup>45</sup>. In this simulation, the static coefficient of friction was 0.5 and the ambient temperature was set at 25 °C.

Potential energy was estimated as follows: The deformed circular shell was divided into  $n$  particles, with  $[x_i, y_i]^T$  being the coordinates of the  $i$ -th particle. If  $M$  is the mass of the robot, and if the entire mass is distributed on the shell, the mass of each particle is given by  $m = M/n$ . Thus, the gravitational potential energy  $\mathcal{U}_{\text{grav}}$  is

$$\mathcal{U}_{\text{grav}} = \sum_{i=1}^n m g y_i \quad (1)$$

where  $g$  is the acceleration of gravity.

Figure 6 shows the simulated configurations of the rolling robot and the gravitational potential energy changes of each using a quasi-static method. The configuration shown in Fig. 6 closely agreed with the configuration shown in Fig. 3. In Fig. 6, the local minimum point shown with the blue dotted line indicates the rotation angle that is measured from the origin at the initial state (0.0s). Note that the local minimum point is shifted as the robot rolls; thus, this local minimum point refers to the angle of rotation. These results indicate that rolling locomotion uses the gradient of a gravitational potential energy. By comparing the results shown in Fig. 6, we found that the potential energy graphs were similar to each other and that the rolling speeds were almost the same. In addition, robot weight had no effect on rolling locomotion on horizontal ground. Thus, it is easier to roll the robot leftward than rightward down the slope because the peak

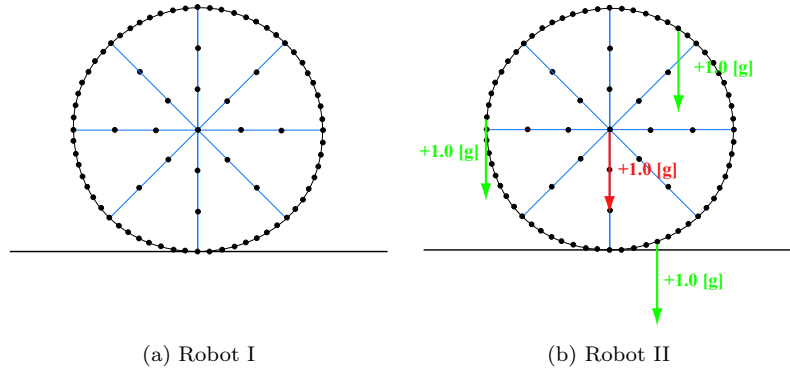


Fig. 5. Particle-based model of a soft robot.

potential energy is on the right half, not on the left half. If the weight is increased, the valley of the potential energy is deepened, and the robot thereby becomes more stable.

The simulated distance moved during rolling locomotion is shown in Fig. 7. We found that the robot behaves in a manner similar to stair-shaped locomotion. Simulation and experimental results were in good agreement, with a margin of error of 2-6% on flat ground and of 4-6% on a slope. The distances traversed by robots I and II coincides with one another, indicating that weight did not significantly affect locomotion. The locomotion distance on a slope was less than that on flat ground due to the slip between robot and ground (Fig. 7-(a) and (b)).

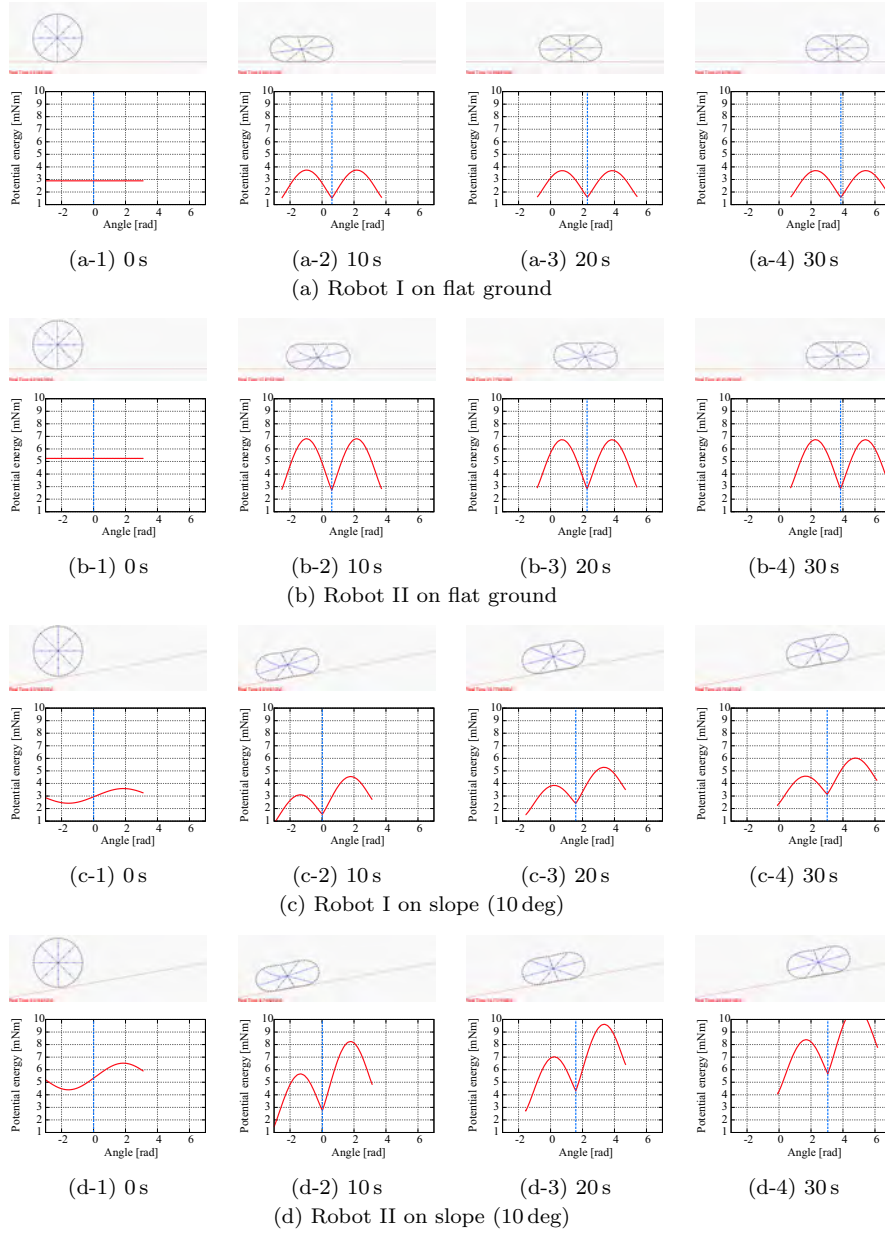


Fig. 6. Simulation results of a rolling soft robot.

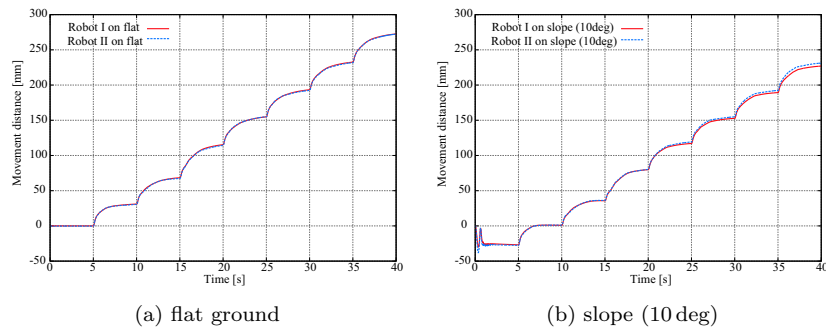


Fig. 7. Simulated distance moved by a rolling soft robot.

## 6. Conclusion

In this paper, we have described the development of a soft robot with a built-in power source. By applying dynamic simulation with particle-based modeling, we analyzed the rolling motion of this robot. This simulation indicated that rolling locomotion uses a gradient of gravitational potential energy. We found that increasing robot weight had almost no influence on its kinematic performance on flat ground, whereas increased robot weight enhanced its stability on inclined ground. These results indicate advantages of attaching sensors to a rolling soft robot. In future experiments, we will apply sensors to the rolling soft robot and try to develop a jumping soft robot with a built-in power source.

## References

1. S. Hirose, *Biologically Inspired Robots - Snake-like Locomotors and Manipulators*, Oxford Science Publications, 1993.
2. Y. Sugiyama, S. Hirai, "Crawling and Jumping of Deformable Soft Robot", *Proc. IEEE/RSJ Int. Conf. on Intelligent Robots and Systems*, pp.3276-3281, Sendai, September, 2004.
3. H. Nakanishi, S. Hirai, "Passive Crawling of a soft robot", *2007 IEEE/ASME Int. Conf. on Advanced Intelligent Mechatronics (AIM2007)*, pp.1-6, ETH Zurich, Switzerland, September. 4-7, 2007 .
4. K. Ikuta, M. Tsukamoto, and S. Hirose, "Mathematical Model and Experimental Verification of Shape Memory Alloy for Designing Micro Actuator", *Proc. of IEEE Micro Electro Mechanical Systems*, pp.103-108, 1991.
5. D. R. Madill, D. Wang, "Modeling and L2-Stability of a Shape Memory Alloy Position Control System", *IEEE Transactions on control systems technology*, Vol.6, No.4, pp.473-481, 1998.